Inelastic tunneling spectroscopy of magnetic tunnel junctions based on CoFeB/MgO/CoFeB with Mg insertion layer

Guo-Xing Miao[a)]
MINT Center, University of Alabama, Tuscaloosa, Alabama 35487 and Physics Department, Brown University, Providence, Rhode Island 02912

Krishna B. Chetry, Arunava Gupta, and William H. Butler
MINT Center, University of Alabama, Tuscaloosa, Alabama 35487

Koji Tsunekawa and David Djayaprawira
Anelva Corporation, 5-8-1 Yotsuya, Fuchu, Tokyo 183-8508, Japan

Gang Xiao
Physics Department, Brown University, Providence, Rhode Island 02912

(Presented on 3 November 2005; published online 18 April 2006)

Magnetic tunnel junctions (MTJs) based on textured MgO barriers have thus far shown the highest tunneling magnetoresistance (TMR) at room temperature. In contrast to traditional magnetic tunnel junctions, it appears that the large TMR observed in these systems arises from a type of coherent tunneling in which the symmetry of the Bloch state wave functions plays a critical role. We have fabricated MTJs with artificial asymmetric barriers by depositing a thin layer of Mg of varying thickness (0–10 Å) prior to the growth of the MgO barrier into otherwise identical CoFeB/MgO/CoFeB MTJs. The inelastic tunnel spectrum shows magnon and phonon excitation peaks similar to traditional Al_2O_3 barriers, and an additional peak at about 300 meV. The conventional interpretation that this peak corresponds to density of states of the *s* electrons in the ferromagnetic electrodes, however, does not apply in the MgO system. © *2006 American Institute of Physics*. [DOI: 10.1063/1.2162047]

Magnetic tunnel junctions have been widely studied for a decade, and they have recently been incorporated in magnetic random access memory (MRAM) devices and magnetic sensors. For these applications, large tunneling magnetoresistance (TMR) ratio and resistance area (*RA*) product in the range of 1–1000 $\Omega\ \mu m^2$ are preferred. There has been a significant amount of work devoted to amorphous AlO_x-based MTJs in the last decade and TMR values as high as 70% were reported.[1,2] Much larger TMR in the single-crystal Fe(001)/MgO(001)/Fe(001) system was predicted by a group of theorists using a theory of coherent tunneling of Bloch states with different symmetry.[3,4] Only recently, a giant leap in MR was reported by various groups in MgO-based MTJs, reaching values as high as 230% at room temperature and *RA* as low as 10 $\Omega\ \mu m^2$.[5–8] The tunneling mechanism in these single-crystalline or textured MgO barriers is fundamentally different from traditional amorphous barrier materials such as AlO_x. One of the most striking differences is that MgO-based MTJs exhibit very little temperature or bias dependence in the parallel moment state (Fig. 1), which is usually a signature of high barrier height. Yet the junctions also show very low *RA* compared to Al_2O_3-based junctions, appearing to have low barrier heights. We will explain these discrepancies based on Ref. 3. Subtle resonance peaks can, however, still be observed when we carefully examine the inelastic tunneling spectrum for parallel moments.

The MTJ stack is deposited onto 3 in. thermally oxidized Si wafers using a commercial magnetron sputtering system (ANELVA C7100) with base pressure less than 5×10^{-9} Torr.[8] The details of the layers in the stack are (in Å): 100 Ta/150 PtMn/25 $Co_{70}Fe_{30}$/8.5 Ru/30 $Co_{60}Fe_{20}B_{20}$/(0–10 Mg)/18 or 25 MgO/30 $Co_{60}Fe_{20}B_{20}$/100 Ta/40 Ru. A thin layer of Mg of varying thickness is deposited prior to the growth of the MgO barrier layer. The wafers are annealed in high vacuum at 360 °C for 2 h and cooled down in a magnetic field for setting the PtMn antiferromagnet. We use optical lithography to pattern the stack and ion milling to define the bottom electrode and the junction area. A 500 Å gold layer is thermally evaporated to serve as the top contact electrode. The dynamic tunneling spectrum dI/dV is obtained using a standard lock-in method at 80 Hz (Stanford SR830 DSP with SR550 preamplifier). A modulation peak to peak voltage of approximately 1–2 mV is used to ensure that there is no modulation broadening. The second derivative d^2I/dV^2 is obtained mathematically from the dI/dV data. Band structures are calculated with generalized gradient approximation (GGA), based on an artificial tetragonal Co_3Fe cell.

Since the CoFeB grows amorphous it forms a smooth layer while also promoting a textured uniform growth of the MgO on top.[8] However, the ferromagnetic electrodes have to be crystallized at least locally for the coherent tunneling to occur through the interface.[3,4] It has been shown that the annealing step is crucial to obtaining high TMR,[8] likely because of the formation of crystallized magnetic layers at the two interfaces. Similar crystallization of CoFeB layers has also been reported in CoFeB–AlO_x-based MTJs.[10] For these

[a)]Electronic mail: miao@physics.brown.edu

 © 2006 American Institute of Physics

Downloaded 20 Apr 2009 to 128.148.60.205. Redistribution subject to AIP license or copyright; see http://jap.aip.org/jap/copyright.jsp

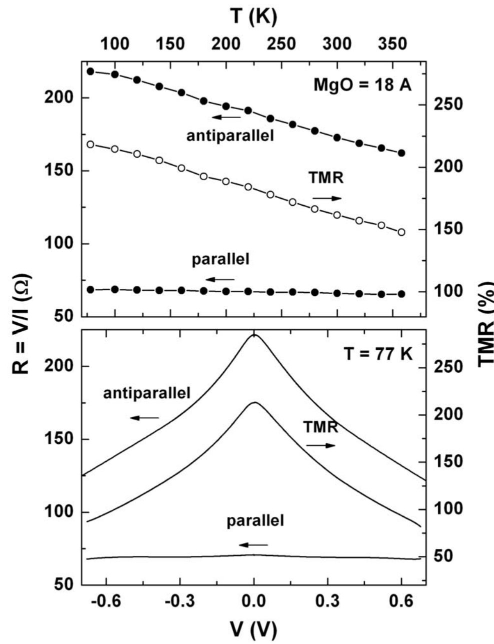

FIG. 1. Temperature and bias dependences of the TMR and junction resistance (R=V/I) in the spin parallel and spin antiparallel configurations.

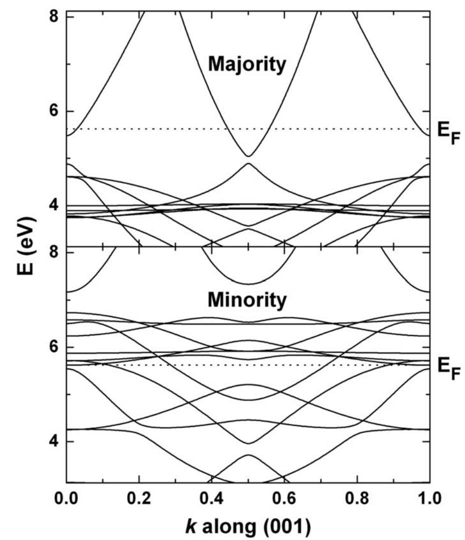

FIG. 2. Band structure of bcc Co_3Fe along the (001) direction. Fermi level is marked with dashed lines.

reasons and for simplicity, we will model our band calculations on bcc Co_3Fe in the following discussions (Fig. 2).

The bands of the majority channel may be thought of loosely as "free-electron" bands. The basic electronic structure of FeCo alloys consists of a highly dispersive free-electron band that begins at the Γ point approximately 4 eV below the *d* bands. Its energy increases rapidly with *k* until it encounters the weakly dispersive (localized, low group velocity) *d* bands at which point it hybridizes and the hybrid band becomes relatively flat. The free-electron band emerges again from the top of the *d*-band complex, approximately 4 eV above where the hybridization began. Because the magnetic moments on the Fe and Co atoms in bcc FeCo alloys differ by 1 μ_B, each atom has the same number of majority electrons. This implies that there is little difference in the atomic potentials seen by the majority electrons and that therefore there is very little scattering of these electrons. Thus the approximation of the majority channel by a periodic system is not unrealistic. The Fermi energy for the majority electrons lies above the *d* bands, so that the only majority Bloch state is the free electron or Δ_1 symmetry state. The major differences between the majority and minority channels are the position of the Fermi energy, which for the minority channel is within a complex of relatively flat *d* bands near the top of the *d*-band complex, and the stronger scattering because of the larger difference in the atomic potentials in the minority channel. The bands near the top of the *d*-band complex are antibonding states which tend to be particularly flat even for *d* bands. The strong scattering due to substitutional disorder may lead to the generation of Δ_1 symmetry.

The most dramatic distinction of the MgO-based MTJ's from all previously reported results is that the spin parallel resistance of the junctions are nearly independent of either bias voltage or temperature (Fig. 1). As a result, the observed bias and temperature dependences of the TMR come almost entirely from the spin antiparallel alignment as predicted by theory.[3,4] We have plotted the TMR result together with the resistance results to manifest this similarity (Fig. 1). As explained by Butler *et al.*,[3] the wave-function decay in the barrier is given by the complex energy bands of the MgO. For parallel moment alignment, the relevant complex energy band is the Δ_1 band given quite accurately by $1/k^2 = [-\hbar^2/2m_\nu(E-E_\nu)] + [\hbar^2/2m_c(E-E_c)]$, where m_ν and m_c are the valence and conduction band masses, respectively, and E_ν and E_c represent the top of the valence band and the bottom of the conduction band. For the case of MgO, the valence and conduction band masses are nearly equal. Further, according to Ref. 3, the Fermi energy lies at midgap where dk/dE vanishes. In MgO, the gap (E_c-E_ν) is approximately 8 eV which is large compared to the 0.5 V range, ΔE over which the parallel resistance is constant. We estimate that over this range k varies as $k \approx k_0\{1-2[(\Delta E)^2/E_C - E_G]\}$ so that the electron decay rate in the barrier changes by less than 1% over the energy range shown in Fig. 1, and that the change in the conductance over this range due to the change in the decay rate is less than 10% for an 18-Å-thick MgO barrier. In summary, the observed flat temperature and bias dependences of spin parallel resistance is an indication of very high tunnel barriers. On the other hand, the experimentally observed low *RA* value is because the decay rate of electrons forming Bloch states in MgO (especially Δ_1 states) is much slower compared to that of free electrons in a simple potential barrier due to the structure of the MgO complex bands. Applying the WKB approximation to MgO systems significantly underestimates the barrier heights.[7]

The dynamic conductance spectrum reveals the detailed excitation states across the barrier even for the nearly flat spin parallel alignment. The basic shape of the conductance $G=dI/dV$ vs V plot (Fig. 3) is a parabola, which we speculate arises from the elastic tunneling contributions.[11] At very low bias, a contribution linear in V can be seen in both the spin parallel and spin antiparallel alignments, and there is also a tendency for the conductance to drop near 300 meV. These inelastic contributions to tunneling can be better seen

Downloaded 20 Apr 2009 to 128.148.60.205. Redistribution subject to AIP license or copyright; see http://jap.aip.org/jap/copyright.jsp

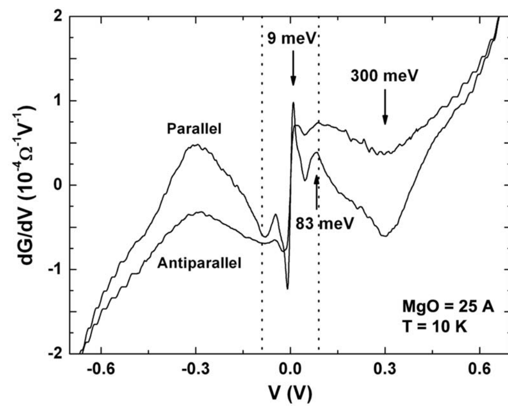

FIG. 3. Inelastic eletrcon tunneling spectrum of a junction with a 25 Å MgO barrier (no Mg insertion layer). The arrows indicate the resonant peak positions and dashed lines indicate the position of $E_m = 3kT_C/(S+1)$.

in the conductance derivative dG/dV vs V plot (Fig. 3). There are magnon excitation peaks visible at low energy around 9 meV, and they have a cutoff energy at about $E_m = 3kT_C/(S+1) \approx 90$ meV, where T_C is the effective Curie temperature at the interface for which we used the CoFe bulk value. At slightly higher energies, a second peak emerges as the electron energy gets high enough to excite phonons in the MgO barrier. The peak position matches closely the Mg–O phonon frequency, which is at 651 cm^{-1} in bulk single crystal MgO[17] and corresponds to an energy level of 80.7 meV. These peaks are universal features for any tunneling junctions and very similar results have been reported in amorphous AlO_x MTJs.[9] A third peak, which tends to decrease conductance at about 300 meV, also has its analogy in the Al_2O_3-based MTJs, and it has been associated with the partial density of states (DOS) of the *s* electrons in the ferromagnetic electrodes.[12,13] However, such argument will not hold in the MgO-based tunneling junctions. Instead, this peak should be a strong indication that some emerging Bloch bands are participating in tunneling at this energy, most likely it is the contribution coming from the highly dispersive bands in the minority channel (Fig. 2), most of which have Δ_5 characteristics.

We fabricated MTJs with a thin layer of Mg insertion, in the same spirit as proposed by Mathon and Umerski[14] and Belashchenko *et al.*[15] for Au/Ag insertion in order to prevent Fe oxidation and to suppress tunneling through mismatched interface bands. The TMR slightly increases with the first few angstrom Mg layer, probably due to the partial conversion of Mg into MgO, then drops significantly with further increase in the Mg layer because a too thick Mg layer will tend to break the coherence between the ferromagnetic electrodes and the barrier (Fig. 4). The *RA* value increase indicates that there is indeed some Mg conversion into MgO, but only by a small amount because a fully oxidized 10 Å Mg (effectively 12.5 Å MgO) will increase *RA* by more than three orders of magnitude.[7] It is not surprising that the first two characteristic peaks in the dG/dV spectrum also show up in these samples even with a 10 Å Mg insertion layer, because the magnon peak is determined by the ferromagnetic electrodes, and the phonon peak is determined by the Mg–O bonding strength.[16] However, the third peak, which likely

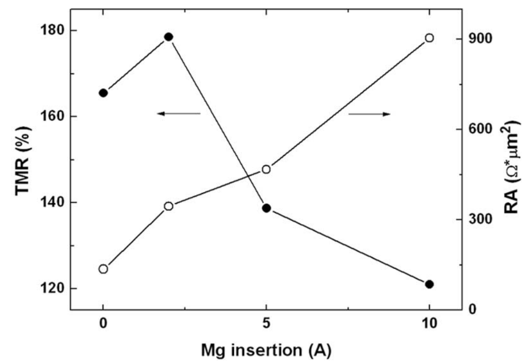

FIG. 4. TMR dependence on the Mg insertion layer thickness at room temperature.

comes from the Δ_5 states, still survives even 10 Å Mg layer. This indicates that Mg, having low atomic number and being loosely lattice matched with Fe and MgO, may maintain the spin symmetry coherence over a much longer distance. The still significantly high TMR in samples with 10 Å Mg provides further confirmation for this argument, and this makes it less demanding in the actual junction fabrications.

In summary, we have fabricated MTJs based on CoFeB/MgO/CoFeB, and studied their dynamic tunneling spectrum. Nearly flat temperature and bias dependence of the spin parallel resistance are attributed to high barrier height, while the low *RA* value is attributed to the slow decay rate of Bloch states in MgO barriers. We have also fabricated similar MTJs with a thin layer of Mg insertion up to 10 Å, and it is interesting that spin coherence can survive even for a 10 Å Mg layer, indicating that the Bloch states have long diffusion length in Mg.

We thank P. LeClaire for his insightful comments and suggestions. The work was supported by the NSF MR-SEC Grant No. DMR0213985 and NSF Grant No. DMR0520491.

[1]S. Tehrani, G. Engel, J. M. Slaughter, E. Chen, M. DeHerrera, M. Durlam, P. Naji, R. Whig, J. Janesky, and J. Calder, IEEE Trans. Magn. **36**, 9464 (2000).
[2]D. Wang, C. Nordman, J. M. Daughton, Z. Qian, and J. Fink, IEEE Trans. Magn. **40**, 2269 (2004).
[3]W. H. Butler, X.-G. Zhang, T. C. Schulthess, and J. M. MacLaren, Phys. Rev. B **63**, 054416 (2001).
[4]J. Mathon and A. Umersky, Phys. Rev. B **63**, 220403(R) (2001).
[5]S. Yuasa, A. Fukushima, T. Nagahama, K. Ando, and Y. Suzuki, Jpn. J. Appl. Phys., Part 2 **43-4B**, L588 (2004).
[6]S. S. P. Parkin, C. Kaiser, A. Panchula, P. M. Rice, B. Hughes, M. Samant, and S.-H. Yang, Nat. Mater. **3**, 862 (2004).
[7]S. Yuasa, T. Nagahama, A. Fukushima, Y. Suzuki, and K. Ando, Nat. Mater. **3**, 868 (2004).
[8]D D. Djayaprawira *et al.*, Appl. Phys. Lett. **86**, 092502 (2005).
[9]T. Dimopoulos, G. Gieres, J. Wecker, Y. Luo, and K. Samwer, Europhys. Lett. **68**, 706 (2004).
[10]S. Cardoso *et al.*, J. Appl. Phys. **97**, 10C916 (2005).
[11]W. F. Brinkman, R. C. Dynes, and J. M. Rowell, J. Appl. Phys. **41**, 1915 (1970).
[12]P. LeClair *et al.*, Phys. Rev. Lett. **88**, 107201 (2002).
[13]A. H. Davis and J. M. MacLaren, J. Appl. Phys. **91**, 7023 (2002).
[14]J. Mathon and A. Umerski, Phys. Rev. B **71**, 220402(R) (2005).
[15]K. D. Belashchenko, J. Velev, and E. Y. Tsymbal, Phys. Rev. B **72**, 140404(R) (2005).
[16]X. F. Han, J. Murai, Y. Ando, H. Kubota, and T. Miyazaki, Appl. Phys. Lett. **78**, 2533 (2001).
[17]P. A. Thiry, M. Liehr, J. J. Pireaux, and R. Caudano, Phys. Rev. B **29**, 4824 (1984).

Downloaded 20 Apr 2009 to 128.148.60.205. Redistribution subject to AIP license or copyright; see http://jap.aip.org/jap/copyright.jsp